Hydrogen production on CoFe, CoFeMn and CoFeMo coatings deposited on Ni foam via electroless metal plating

Huma Amber[*],

Karina Vjūnova,

Zita Sukackienė,

Dijana Šimkūnaitė,

Jūratė Vaičiūnienė,

Loreta Tamašauskaitė-Tamašiūnaitė[*],

Eugenijus Norkus

Department of Catalysis,
Center for Physical Sciences
and Technology (FTMC),
3 Saulėtekio Avenue,
10257 Vilnius, Lithuania

In this study, the catalytic hydrogen generation was evaluated on the cobalt–iron (CoFe), cobalt–iron–manganese (CoFeMn) and cobalt–iron–molybdenum (CoFeMo) coatings deposited on the Ni foam substrate using the electroless metal plating method and morpholine borane as the reducing agent. The characterisation of the surface morphology, structure and composition of resulted coatings was done using scanning electron microscopy (SEM) and inductively coupled plasma optical emission spectroscopy (ICP-OES). The catalytic activity of the prepared CoFe/Ni, CoFeMn/Ni and CoFeMo/Ni catalysts was investigated for hydrogen generation from an alkaline sodium borohydride ($NaBH_4$) solution at different temperatures. It was found that the hydrogen generation rate of ca. 5.2, 7.8 and 11.7 L min^{-1} g^{-1} was achieved by using the CoFe/Ni, CoFeMo/Ni and CoFeMn/Ni coatings, respectively, at 343 K. Among the investigated catalysts, CoFeMn/Ni exhibits the lowest activation energy of 62.4 kJ mol^{-1} and the highest HGR of 11.7 L min^{-1} g^{-1} at 343 K.

Keywords: hydrogen generation, cobalt, iron, molybdenum, manganese, electroless metal plating, morpholine borane

INTRODUCTION

Given the global energy crisis, efficient hydrogen (H_2) production is becoming one of the driving forces behind the H_2 economy and sustainable development. However, most of today's H_2 is produced by steam methane reforming and coal gasification, both of which emit CO_2 and require carbon capture and storage to reduce the environmental impact [1, 2]. Clean H_2 production and storage is a vital and commercially viable alternative. H_2 can be produced from a variety of renewable energy sources such as solar, wind, geothermal and tidal power, as well as from state-of-the-art H_2 production methods such as water electrolysis, including photocatalytic/photo-electrochemical water splitting or hydrolysis of hydrogen-rich substances [3–5]. The latter, in the form of on-site H_2 generation by hydrolysis of lightweight materials, is of particular interest as it allows mitigating the challenge of H_2 storage in a simple and efficient manner [6, 7]. Due to its potentially explosive nature, a compact, safe and efficient means of storing H_2 is required [6]. Thus, hydrolysis of light metals and hydrides can be efficiently used to produce H_2 locally in fuel cell vehicles or, alternatively, to fill their fuel tanks with locally produced and compressed H_2 at near ambient conditions without a compressor [8]. Recently, a lot of attention has been paid to H_2 production by hydrolysis of metal hydrides, mainly due to the high theoretical H_2 yield, low energy consumption and catalyst

[*] Corresponding author. E-mail: huma.amber@ftmc.lt;
loreta.tamasauskaite@ftmc.lt

costs, and simple operating conditions at elevated gravimetric H_2 capacity of about 10% w/w [9, 10]. Heavy metal-based hydrides, including $TiFeH_2$, $LaNi_5H_{6.7}$, Mg_2NiH_4, $NaAlH_4$, etc., have also been thoroughly investigated, but compared to light metal hydrides, $NaBH_4$, MgH_2, CaH_2 and $LiBH_4$ are disadvantaged by severe H_2 supply operating conditions.

Meanwhile, light metal hydrides are inferior due to the formation of surface passivation layers, resulting in lower reaction kinetics. However, their low cost makes them the most suitable ones for industrial use. Among these, sodium borohydride ($NaBH_4$) is the most extensively studied metal hydride due to its controllability and safety, as well as its high gravimetric hydrogel density of 10.8 wt% and ability to produce H_2 by hydrolysis at ambient conditions [11–12]. $NaBH_4$ can release H_2 via the hydrolysis reaction by Eq. (1), where $NaBH_4$ reacts with water to produce H_2 and sodium metaborate ($NaBO_2$) [5, 9]:

$$NaBH_4 + 2H_2O \rightarrow NaBO_2 + 4H_2. \qquad (1)$$

However, the kinetics of this reaction are relatively slow [11]. Developing efficient catalysts is critical to ensure high H_2 production rates for practical use. Many homogeneous and heterogeneous catalysts have been developed to speed up the production of H_2 gas via this reaction [13]. Among these, noble metal or noble metal-based catalysts such as Ru [14], Pt [15], Pd [16] and Au [17] have been the research focus due to their stable chemical properties and superior catalytic activity towards $NaBH_4$ hydrolysis. However, their high cost and limited reserves prevent their widespread use and commercial applications. Transition metal catalysts have been developed as affordable and reasonably priced substitutes for expensive precious metals. So far, cobalt-based materials have proved to be superior catalysts for the hydrolysis of $NaBH_4$ [18, 19]. They can act effectively as single metal catalysts, for example, as ultrafine cobalt nanoparticles supported on carbon nanospheres (CNSs@Co) [20], Co-anchored on nanoporous graphene oxide (Co/PGO) [21], or Co-B based [22], etc. Despite the enormous efforts made to develop cobalt and cobalt-supported catalysts with high-performance catalytic activity, the main drawback is the deactivation of

the catalysts by a thick passivation layer of B–O-based compounds. Creating mixed cobalt systems with different metals reduces or even prevents adsorbed borate formation. Coupling with other elements such as Ni, Cu, Mo, Mn and Fe in the form of bimetallic Co–Ni [23, 24], Co–Fe [25, 26], ternary Ni–Co–Mn, Co–Cu–Ni [23, 27], quaternary Co–Mo–Ru–B [28], Ni–Co–Mo–Mn [23] or even in the form of multi-element compounds such as Co–Ni–Mo–P/g–A_2O_3 [29] has led to a significant improvement in catalyst functionality as a result of the synergistic interactions of different metals. In addition, doping with other metals has made it possible to effectively disperse the catalysts on the surface and increase their contact area with the reactants. For example, the Fe–Co–B catalyst [30] showed a better catalytic activity towards $NaBH_4$ dehydrogenation than the analogous Co–B material (4536 vs 1869 mL min^{-1} g_{cat}^{-1}) due to the ability of Fe to act as a promoter and allow a better dispersion of the particles.

However, the typical phenomenon of particle aggregation or agglomeration, resulting in a reduced number of exposed active sites, is one of the reasons for a poor catalytic performance. Suitable support materials with high surface areas have to be used to address this problem and increase the H_2 generation rate (HGR). A number of materials have been successfully used as supports, including various forms of carbon (activated carbon, carbon nanotubes, or graphitic carbon nitrides) [25, 31], Ni foam [31, 32], metal oxides [29], or metal-organic frameworks (MOFs) [26]. Due to their porous structure and usually large surface area, they suppress the agglomeration of active sites, facilitate the sorption of reactants and thus surface reaction, and ensure an effective mass transfer. Cost-effective and efficient non-noble metal catalysts for catalytic H_2 production are a significant challenge. Herein, we present efficient non-noble catalysts – the CoFe, CoFeMn and CoFeMo coatings deposited on the Ni foam substrate, for the catalytic H_2 production from an aqueous $NaBH_4$ solution. Moreover, the low-cost and straightforward electroless metal plating method was used to fabricate catalysts. The catalytic activity of the CoFe/Ni, CoFeMn/Ni and CoFeMo/Ni catalysts was investigated for H_2 generation from an alkaline $NaBH_4$ solution at different temperatures.

EXPERIMENTAL

$CoSO_4 \cdot 7H_2O$ (99.5%, Sigma-Aldrich), $Na_2MoO_4 \cdot 2H_2O$ (99.5%, Chempur), $FeSO_4 \cdot 7H_2O$ (99.0%, Eurochemicals), $MnSO_4 \cdot H_2O$ (99.0%, Chempur), NH_2CH_2COOH (99.0%, Sigma-Aldrich), $C_4H_8ONH \cdot BH_3$ (97.0%, Alfa Aesar), $NaBH_4$ (96.0%, Sigma-Aldrich), NaOH (98.8%, Chempur), $PdCl_2$ (59.5% Pd, Alfa Aesar), HNO_3 (65.0%, Chempur) and HCl (35–38%, Chempur) were analytical grade and used without any further treatments. The nickel (Ni) foam with 20 pores cm^{-1}, a bulk density of 0.45 g cm^{-3} and a thickness of 1.6 mm (Goodfellow GmbH) was used as a substrate for Co coatings.

Co binary and ternary coatings, CoFe, CoFeMn and CoFeMo, were deposited on Ni foam (1 × 1 cm) using the electroless metal deposition method using morpholine borane (MB) as a reducing agent. At first, the Ni foam was pretreated in a HCl : H_2O (1 : 1 vol) solution at room temperature for 1 min, thoroughly rinsed with distilled water and dried. Then, the pre-treated Ni foam was dipped in a 0.5 g L^{-1} $PdCl_2$ solution for 1 min, washed with distilled water, dried and placed into a plating bath. The plating bath compositions and deposition parameters of binary and ternary Co coatings are given in Table 1. The deposition time and temperature were different in the case of each coating. Moreover, the CoFeMo coating was obtained using two stages by depositing at first the CoMo coating on the Ni foam, followed by the deposition of CoFe.

The composition of the Co-based coatings deposited on the Ni foam was determined using a spectrometer OPTIMA 7000DV (Perkin Elmer, Waltham, MA, USA). The characterisation of the surface morphology and structure of the prepared catalysts was done using a scanning electron microscope 4000TMPlus (Hitachi).

The catalytic activity of the prepared CoFe/Ni, CoFeMo/Ni and CoFeMn/Ni catalysts for H_2 generation was examined in the solution containing 5 wt.% $NaBH_4$ + 0.4 wt.% NaOH at different temperatures (313–343 K). The volume of the released H_2 catalysed by the prepared catalysts was measured using a MilliGascounter (Type MGC-1 V3.2 PMMA, Ritter, Germany) connected to a personal computer. For collecting the generated H_2 gas, a thermostated airtight flask fitted with an outlet connected to the MilliGascounter was used. The investigated catalysts were placed in an alkaline sodium borohydride solution of designated temperature and stirred with a magnetic stirrer.

RESULTS AND DISCUSSION

CoFe, CoFeMn and CoFeMo coatings were investigated as a catalytic material for H_2 generation from alkaline $NaBH_4$ solution. CoFe, CoFeMn and CoFeMo coatings were deposited on the Ni foam surface using the low-cost and straightforward electroless metal plating method. The composition of the Co-based coatings deposited on the Ni foam was determined using inductively coupled plasma optical emission spectroscopy (ICP-OES). The obtained results are mentioned in Table 2.

Figure 1 presents the SEM images of CoFe/Ni, CoFeMn/Ni and CoFeMo/Ni catalysts at different magnifications. As evident from the SEM images in Fig. 1a, the Ni foam is evenly coated with the CoFe coating consisting of globular granules (Fig. 1a'). It can also be observed that the CoFe

Table 1. Composition of plating baths and deposition parameters

Coating		Composition of the plating bath, mol L^{-1}						Deposition conditions		
		$CoSO_4 \cdot 7H_2O$	$C_4H_8ONH \cdot BH_3$	$Na_2MoO_4 \cdot 2H_2O$	$FeSO_4 \cdot 7H_2O$	$MnSO_4 \cdot H_2O$	Glycine	T, °C	t, min	Solution pH
CoFe/Ni		0.010	0.060	–	0.150	–	0.300	60	30	5
CoFeMn/Ni		0.070	0.060	–	0.005	0.015	0.200	50	15	7
CoFeMo/Ni	1 stage: CoMo	0.010	0.200	0.001	–	–	–	60	2	7
	2 stage: CoFe	0.010	0.060	–	0.150	–	0.300	60	30	5

Table 2. Composition of CoFe, CoFeMo and CoFeMn coatings deposited on the Ni foam

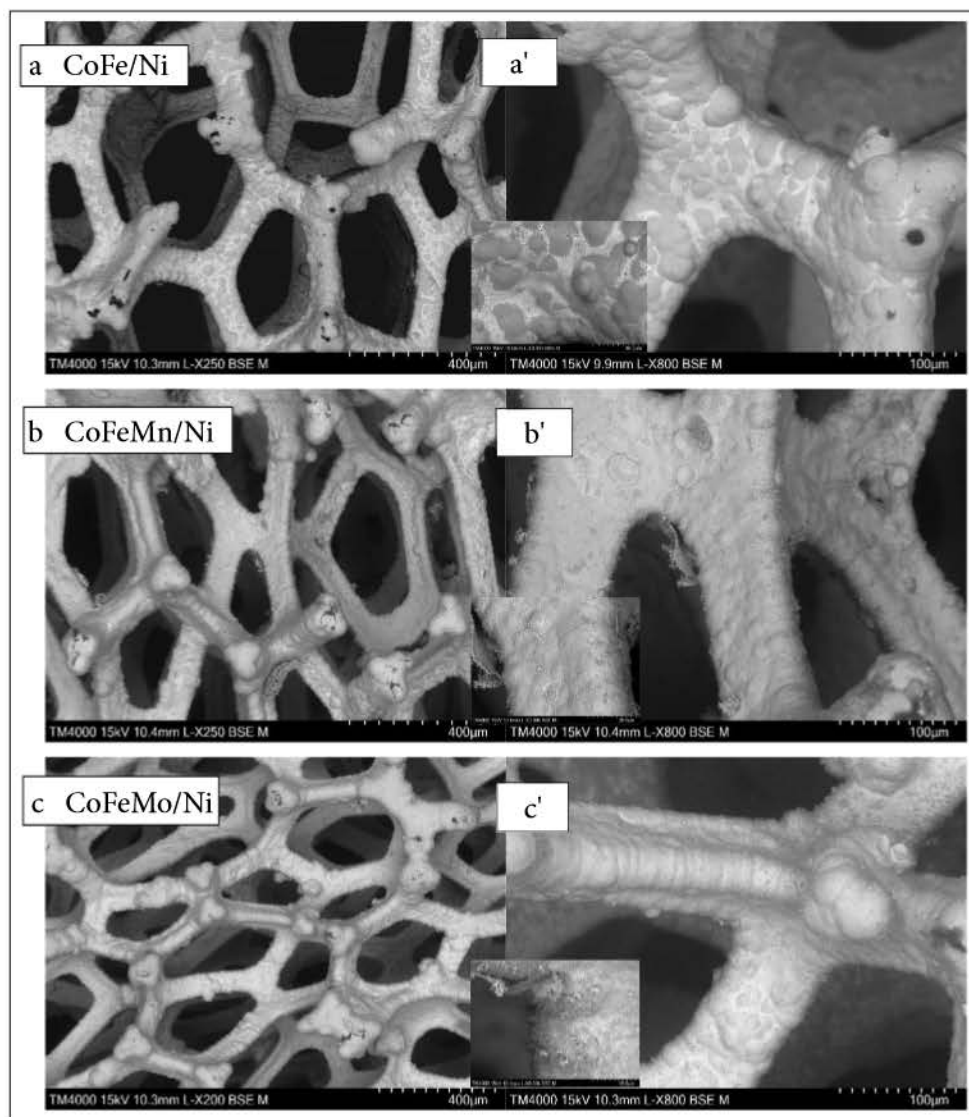| Catalyst	Composition, wt.%				Total catalyst loading, $mg_{cat}\ cm^{-2}$
	Co	Mn	Mo	Fe	
CoFe/Ni	31.92	–	–	68.08	0.49
CoFeMo/Ni	82.04	–	6.21	11.74	1.13
CoFeMn/Ni	95.45	0.49	–	4.06	2.00

Fig. 1. SEM images of the CoFe (a, a′), CoFeMn (b, b′) and CoFeMo (c, c′) coatings deposited on the Ni foam at different magnifications

coating is composed of crystallites in a size of 10–11 µm. The SEM images in Fig. 1b, b′ and c, c′ clearly show that the Ni foam is also uniformly coated with the CoFeMn and CoFeMo coatings, which are compact, uniform, without cracks and any defects, and consist of much finer and denser crystallites (3–4 µm) than the CoFe coating (Fig. 1a).

Further, the hydrolysis of $NaBH_4$ was examined on the CoFe/Ni, CoFeMo/Ni and CoFeMn/Ni catalysts. Figure 2 presents the temperature-time-dependent volume of generated H_2 (mL) from the $NaBH_4$ solution obtained on the CoFe/Ni (a), CoFeMo/Ni (b) and CoFeMn/Ni (c) catalysts at different temperatures.
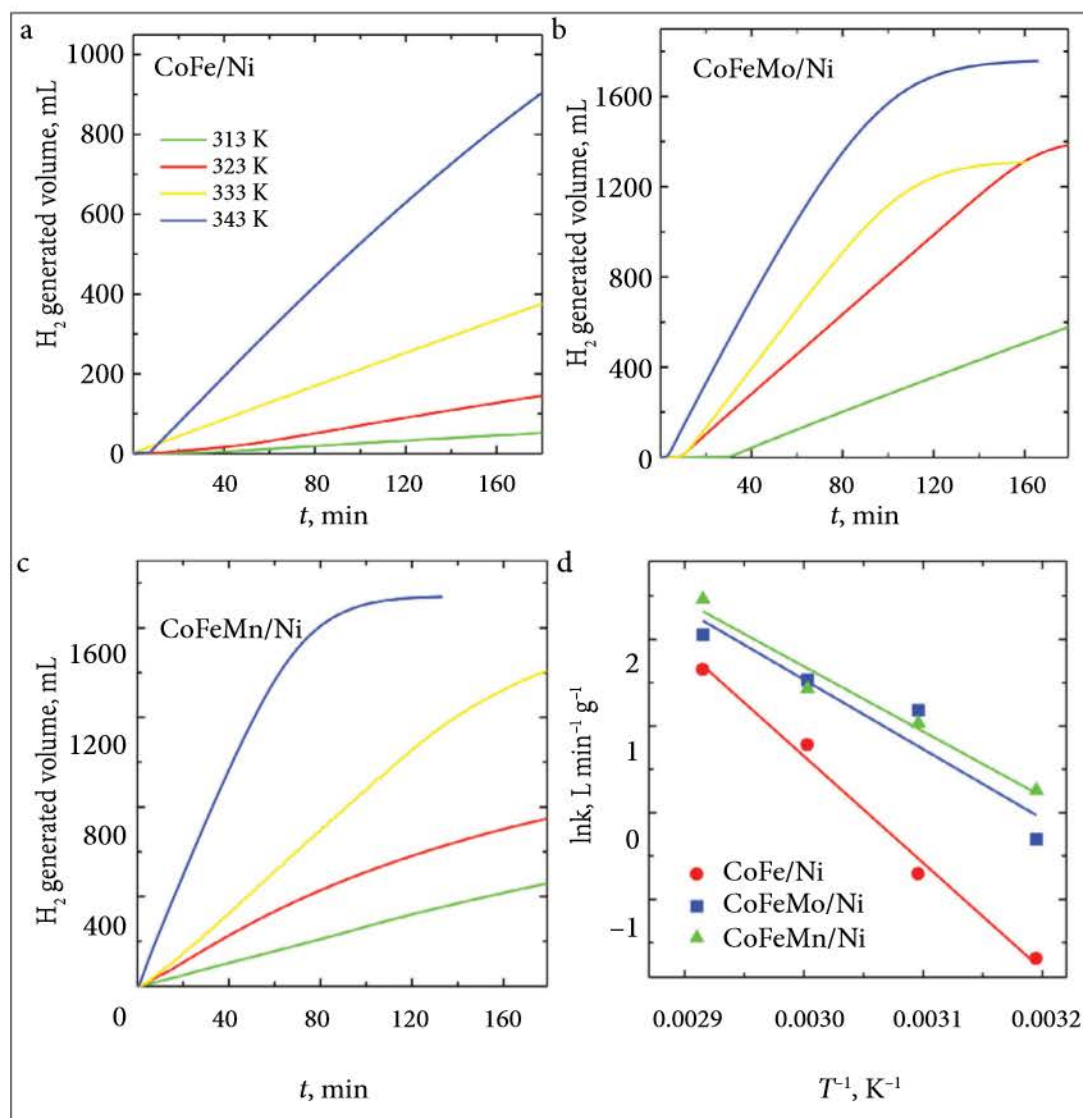
Fig. 2. H$_2$ generation from the 5 ml 5 wt% NaBH$_4$ + 0.4 wt% NaOH solution, catalysed by the CoFe/Ni (a), CoFeMo/Ni (b) and CoFeMn/Ni (c) catalysts at different temperatures. (d) The corresponding Arrhenius plots

It can be seen that the generated H$_2$ volume increases with the increase in temperature on all investigated catalysts. The summarised data for the HGR are given in Table 3 and Fig. 3. HGR exponentially increases with the rise in temperature. When the temperature enhanced from 313 to 343 K, the HGR for the CoFe/Ni catalyst was also enhanced from 0.2 to 5.2 L min^{-1} g$_{cat}$$^{-1}$, for the CoFeMo/Ni catalyst from 0.7 to 7.8 L min^{-1} g$_{cat}$$^{-1}$ and for the CoFeMn/Ni coating from 1.3 to 11.7 L min^{-1} g$_{cat}$$^{-1}$. Furthermore, the highest HGR was measured at 34 K on the CoFe/Ni, CoFeMo/Ni and CoFeMn/Ni catalysts: 5.2, 7.8 and 11.7 L min^{-1} g$_{cat}$$^{-1}$, respectively.

The activation energy (E_a) of the hydrolysis reaction of NaBH$_4$ was determined by using the Ar-

rhenius equation based on the ln(k) versus $1/T$ dependence according to Eq. (2),

$$E_a = \frac{\Delta \ln k}{\Delta \frac{1}{T}} * R,$$

(2)

where E_a is the activation energy (J), R is the general gas constant (8.314 J mol^{-1} K^{-1}), k is the reaction rate coefficient, and T is the temperature (K).

Arrhenius plots of ln(k) vs $1/T$ were constructed from the data presented in Fig. 2a–c and are illustrated in Fig. 2d. Based on those data, E_a values were determined to be 62.4, 66.8 and 102.6 kJ mol^{-1} for CoFeMn/Ni, CoFeMo/Ni and CoFe/Ni (Table 3). It should be noted that the activation

Table 3. Hydrogen generation rates and activation energies on the deposited catalysts at different temperatures

Catalyst	E_a, kJ mol^{-1}	T, K	HGR, L min^{-1} g$_{cat}^{-1}$
CoFe/Ni	102.6	313	0.2
		323	0.5
		333	2.2
		343	5.2
CoFeMo/Ni	66.8	313	0.7
		323	3.3
		333	4.6
		343	7.8
CoFeMn/Ni	62.4	313	1.3
		323	2.8
		333	4.2
		343	11.7

Fig. 3. Hydrogen generation rate on the Co coatings at 313–343 K

energies for CoFeMn/Ni and CoFeMo/Ni are always lower when compared to those of pure CoFe/Ni (102.6 kJ mol^{-1}). The favourable activation energy values obtained in the present work may be attributed 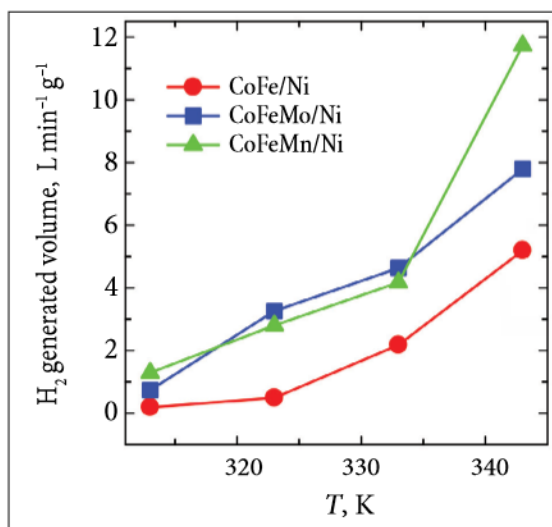to promoting effects, caused by the co-deposition of different transition metals – Mn and Mo with CoFe, to enhance the catalytic hydrolysis reaction. Among the investigated catalysts, the CoFeMn/Ni catalyst has the lowest activation energy of 62.4 kJ mol^{-1} and the highest HGR of

Table 4. Comparison of HGRs and activation energies for different catalysts

Catalyst	T, K	HGR, L min^{-1} g$_{cat}^{-1}$	E_a, kJ mol^{-1}	Electrolyte	References
Co	–	–	75	–	[33]
Ni	–	–	71	–	[33]
Raney Ni	–	–	63	–	[33]
CoBMo/Cu	343	–	27	5 wt% NaBH$_4$ + 0.4 wt% NaOH	[34]
CoBMn/Cu	343	–	48	5 wt% NaBH$_4$ + 0.4 wt% NaOH	[34]
CoBZn/Cu	343	–	71	5 wt% NaBH$_4$ + 0.4 wt% NaOH	[34]
CoFeB/Cu	343	–	74	5 wt% NaBH$_4$ + 0.4 wt% NaOH	[34]
Fe–Co–B	303	4.536	38.9	5% NaBH$_4$ + 1% NaOH	[30]
	333	13.960	38.9	5% NaBH$_4$ + 1% NaOH	
Fe–Co–B/Ni foam	303	22.0	27	15 wt% NaBH$_4$ + 5 wt% NaOH	[35]
Co–W–B/Ni foam	303	15.0	29	20 wt% NaBH$_4$ + 5 wt% NaOH	[36]
Co–B$_{bubble}$	313	5.31	30	1 wt% NaBH$_4$ + 1 wt% NaOH	[37]
Co/Fe$_3$O$_4$@GO	313	6.005	44.4	5.135 wt% NaBH$_4$	[25]
Co-B/Ni foam	298	11.0	33	20 wt% NaBH$_4$ + 5 wt% NaOH	[38]
Co@Ni foam	296±0.5	2.650	60±2	38 mg NaBH$_4$ in 1 mL of 4.5 wt% NaOH	[39]
Co–Fe–B	298	10.690	55.6	–	[40]
Co$_3$O$_4$ commercial		0.860	77.9	10 wt% NaBH$_4$ + 8 wt% NaOH	[41]
g-C$_3$N$_4$/Co–Mo–B/Ni foam	298	9.995	52.6	–	[31]
CoFe/Ni	343	5.2	102.6	5 wt% NaBH$_4$ + 0.4 wt% NaOH	In this study
CoFeMo/Ni	343	7.8	66.8	5 wt% NaBH$_4$ + 0.4 wt% NaOH	In this study
CoFeMn/Ni	343	11.7	62.4	5 wt% NaBH$_4$ + 0.4 wt% NaOH	In this study

11.7 L min^{-1} g^{-1} at 343 K. This indicates the high activity of CoFeMn/Ni catalyst as compared with those of the CoFeMo/Ni and CoFe/Ni catalysts.

The comparison of the HGRs and E_a values of the as-prepared catalysts with other catalysts reported in the literature can also be found in Table 4. The E_a values for CoFeMn/Ni and CoFeMo/Ni are also lower than those found for different bulk metal catalysts, such as Co (75 kJ mol^{-1}), Ni (71 kJ mol^{-1}), Raney Ni (63 kJ mol^{-1}) [33] and ternary Co-based catalysts, such as CoBZn/Cu (71 kJ mol^{-1}) and CoFeB/Cu (74 kJ mol^{-1}) [34], whereas the HGRs values are comparable to those obtained with other catalysts (Table 4).

CONCLUSIONS

The low-cost and straightforward electroless metal plating method was used to fabricate efficient CoFe/Ni, CoFeMo/Ni and CoFeMn/Ni catalysts for H$_2$ production from alkaline NaBH$_4$ solutions. The deposited CoFeMo and CoFeMn coatings on the Ni foam are compact, uniform, without cracks and any defects, and consist of much finer and denser crystallites (3–4 μm) than the CoFe coating (10–11 μm). The hydrogen generation rate of ca. 5.2, 7.8 and 11.7 L min^{-1} g^{-1} was achieved by using the CoFe, CoFeMo and CoFeMn coatings, respectively, at 343 K. Among the investigated catalysts, CoFeMn/Ni exhibits the lowest activation energy of 62.4 kJ mol^{-1} and the highest HGR of 11.7 L min^{-1} g^{-1} at 343 K. The obtained CoFeMn/Ni catalyst is a promising candidate for H$_2$ production from an alkaline NaBH$_4$ solution due to its easy preparation, high hydrogen generation rate and low activation energy.

References

1. Hydrogen to the rescue, Nat. Mater., **17**, 565 (2018) [CrossRef] [PubMed].
2. Hydrogen Council, *Hydrogen Insights: A Perspective on Hydrogen Investment, Market Development and Cost Competitiveness*, Hydrogel Council; McKinsey & Company, Hong Kong, China (2021).
3. M. Aravindan, G. Praveen Kumar, *Results Eng.*, **20**, 101456 (2023).
4. D. Kumar, J. E. Abraham, M. Varghese, J. George, M. Balachandran, J. Cherusseri, *Int. J. Hydrogen Energy*, in press [https://doi.org/10.1016/j.ijhydene.2023.07.257].
5. D. Tang, G.-L. Tan, G.-W. Li, et al., *J. Energy Storage*, **64**, 107196 (2023).
6. L. Ouyang, M. Liu, K. Chen, et al., *J. Alloys Compd.*, **910**, 164831 (2022).
7. M. V. Lototskyy, M. W. Davids, T. K. Sekgobela, et al., *Inorganics*, **11**, 319 (2023).
8. T. Hiraki, N. Okinaka, H. Uesugi, T. Akiyama, in: *Materials Issues in a Hydrogen Economy*, pp. 54–61, World Scientific, Singapore (2009).
9. N. S. Muhammed, A. O. Gbadamosi, E. I. Epelle, et al., *J. Energy Storage*, **73**, 109207 (2023).
10. X. Xie, C. Ni, B. Wang, et al., *J. Alloys Compd.*, **816**, 152634, (2020).
11. U. B. Demirci, *Int. J. Hydrogen Energy*, **48**, 29682 (2023).
12. M. Dragan, *Catalysts*, **12**, 356 (2022).
13. H. N. Abdelhamid, *Int. J. Hydrogen Energy*, **46**, 726 (2021).
14. D. D. Tuan, K-Y. A. Lin, *Chem. Eng. J.*, **351**, 48 (2018).
15. Z. Liu, B. Guo, S. H. Chan, E. H. Tang, L. Hong, *J. Power Sources*, **176**, 306 (2008).
16. S. K. Singh, Y. Iizuka, Q. Xu, *Int. J. Hydrogen Energy*, **36**, 11794 (2011).
17. A. Zabielaitė, A. Balčiūnaitė, I. Stalnionienė, et al., *Int. J. Hydrogen Energy*, **43**, 23310 (2018).
18. F. Xu, J. Ren, J. Ma, et al., *Int. J. Hydrogen Energy*, in press [https://doi.org/10.1016/j.ijhydene.2023.08.142].
19. U. B. Demirci, P. Miel, *Phys. Chem. Chem. Phys.*, **16**, 6872 (2014).
20. H. Zhang, G. Xu, L. Zhang, et al., *Renew. Energy*, **162**, 345 (2020).
21. H. Zhang, X. Feng, L. Cheng, X. Hou, Y. Li, S. Han, *Colloids Surf. A Physicochem. Eng. Asp.*, **563**, 112 (2019).
22. N. Patel, A. Miotello, *Int. J. Hydrogen Energy*, **40**, 1429 (2015).
23. Z. Sukackienė, G. Valeckytė, V. Kepenienė, et al., *Coatings*, **13**, 1740 (2023).
24. Ö. Şahin, D. Kılınç, C. Saka, *J. Energy Inst.*, **89**, 617 (2016).
25. F. Mirshafiee, M. Rezgei, *Int. J. Hydrogen Energy*, **48**, 32356 (2023).
26. M. A. de Oliveira, E. S. Souza, J. de J. Santana, et al., *Appl. Surf. Sci.*, **628**, 157361 (2023).
27. X. Wang, Y. Zhao, X. Peng, et al., *Int. J. Hydrogen Energy*, **41**, 219 (2016).
28. W. Wang, Y. Zhao, D. Chen, X. Wang, X. Peng, J. Tian, *Int. J. Hydrogen Energy*, **39**, 16202 (2014).
29. L. Wang, Z. Li, P. Zhang, G. Wang, G. Xie, *Int. J. Hydrogen Energy*, **41**, 1468 (2016).
30. A. Balbay, N. Selvítepe, C. Saka, *Int. J. Hydrogen Energy*, **46**, 425 (2021).

31. J. Ren, J. Ma, F. Xu, et al., *Int. J. Hydrogen Energy* [https://doi.org/10.1016/j.ijhydene.2023.09.110].

32. Y. Wei, M. Wang, W. Fu, et al., *Mater. Lett.*, **308**, 131166 (2022).

33. C. M. Kaufman, B. Sen, *J. Chem. Soc., Dalton Trans.*, **2**, 307 (1985).

34. A.Balčiūnaitė, Z. Sukackienė, K. Antanavičiūtė, et al., *Int. J. Hydrogen Energy*, **46(2)**, 1989 (2021).

35. Y. Liang, P. Wang, H. B. Dai, *J. Alloys Compd.*, **491(1–2)**, 359 (2010).

36. H. B. Dai, Y. Liang, P. Wang, et al., *Int. J. Hydrogen Energy*, **33(16)**, 4405 (2008).

37. X. Wang, J. Liao, H. Li, et al., *Int. J. Hydrogen Energy*, **43**, 17543 (2018).

38. H.-B. Dai, Y. Liang, P. Wang, H. M. Cheng, *J. Power Sources*, **177**, 17 (2008).

39. M. Paladini, G. M. Arzac, V. Godinho, M. C. J. D. Haro, A. Fernández, *Appl. Catal. B: Environ.*, **158–159**, 400 (2014).

40. Y. Wang, D. Zhang, X. Wang, et al., *Mater. Lett.*, **12**, 100104 (2021).

41. W. Niu, D. Ren, Y. Han, Y. Wu, X. Gou, *J. Alloys Compd.*, **543**, 159 (2012)

Huma Amber, Karina Vjūnova, Zita Sukackienė, Dijana Šimkūnaitė, Jūratė Vaičiūnienė, Loreta Tamašauskaitė-Tamašiūnaitė, Eugenijus Norkus

VANDENILIO GAVIMAS ANT CoFe, CoFeMn IR CoFeMo DANGŲ, NUSODINTŲ ANT Ni KIETŲJŲ PUTŲ, TAIKANT CHEMINĮ METALŲ NUSODINIMĄ

Santrauka

CoFe, CoFeMo ir CoFeMn dangos buvo nusodinamos ant Ni kietųjų putų, naudojant cheminį metalų nusodinimo metodą. Suformuotų CoFe/Ni, CoFeMo/Ni ir CoFeMn/Ni katalizatorių paviršiaus morfologija, struktūra bei sudėtis buvo ištirta, naudojant skenuojantį elektroninį mikroskopą (SEM) ir induktyviai susietos plazmos optinės emisijos spektrometrą (ICP-OES), o jų katalizinis aktyvumas buvo įvertintas vandenilio išskyrimui iš vandeninių natrio borhidrido tirpalų. Nustatyta, kad nusodintos CoFeMo ir CoFeMn dangos ant Ni kietųjų putų yra kompaktiškos, tolygios, be įtrūkimų ir jokių defektų, ir susideda iš daug smulkesnių ir tankesnių kristalitų (3–4 µm dydžio) nei CoFe danga (10–11 µm). Išmatuotas vandenilio išsiskyrimo greitis yra apytiksliai 5,2, 7,8 ir 11,7 L min⁻¹ g⁻¹ ant, atitinkamai, CoFe/Ni, CoFeMo/Ni ir CoFeMn/Ni katalizatorių, esant 343 K temperatūrai. Be to, mažiausia aktyvavimo energija – 62,4 kJ mol⁻¹ bei didžiausias vandenilio išsiskyrimo greitis – 11,7 L min⁻¹ g⁻¹, esant 343 K temperatūrai, buvo gauti ant CoFeMn/Ni katalizatoriaus.